Proteomic of lipid rafts in the exocrine pancreas from diet-induced obese rats

Amine Adda Berkane, Hang Thi Thu Nguyen, Fabrice Tranchida, Abdul Waheed, Valérie Deyris, Léopold Tchiakpe, Caroline Fasano, Cendrine Nicoletti, Véronique Desseaux, El Hassan Ajandouz, et al.

Proteomic of lipid rafts in the exocrine pancreas from diet-induced obese rats

Amine Adda Berkane [a], Hang Thi Thu Nguyen [a,b], Fabrice Tranchida [a], Abdul A. Waheed [c], Valérie Deyris [a], Léopold Tchiakpe [d], Caroline Fasano [a], Cendrine Nicoletti [a], Véronique Desseaux [a], El Hassan Ajandouz [a], Danielle Comeau [a], Louis Comeau [a], Abel Hiol [a,*]

[a] *Université Paul Cézanne, FST-Institut Méditerranéen de Recherche en Nutrition IMRN, UMR INRA 1111/PNV UMR 6153 1147, Marseille, France*
[b] *Division of Digestive Diseases, 615 Michael Street, Suite 201 Emory University, Atlanta GA, USA*
[c] *HIV Drug Resistance Program, NCI-NIH, Frederick, MD-21702, USA*
[d] *Laboratoire de Nutrition-Diététique, Université de Méditerranée, France*

Abstract

In the present work, we induced obesity in rats with high-energy-starch diet and studied exocrine pancreas response. The zymogen granule (ZG) or purified plasma membrane (PM) from the exocrine pancreas was used for the isolation of the detergent-resistant membranes (DRMs). Based on high content of cholesterol, GM1, the bile salt dependent lipase (BSDL), and GP2 enrichment, the low-density fractions were defined as lipid rafts. Additionally, the rafts vesicles were determined by immunogold labeling with anti BSDL. By combining MALDI-TOF/MS and nano-LC ESI Q-TOF MS/MS proteomic identification we have selected 33 proteins from the lipid rafts which were classified into at least four functional families. Our data suggest that the acinar PM from the diet-induced obesity rats may be organized into lipid rafts, and characterization of rafts proteome can contribute to improve our understanding of food digestion under obesity.

Keywords: Starch; Diet; Obese; Pancreas; Rafts; Proteomic; BSDL; GP2

The exocrine pancreas is the major source of enzymes responsible for food digestion in the small intestine and its enzymatic adaptations to the diet composition has been reported [1]. Digestive enzymes in the acinar cells are stored in membrane vesicles called zymogen granules (ZGs). While the ZGs formation has been well-studied, their fusion to the PM and the regulation of digestive enzymes secretion from the apical acinar cells remain poorly understood. Our recent understanding of cell membranes suggest that the PM may be organized into heterogeneous functional microdomains and one of such microdomains known as lipid rafts are enriched in glycosphingolipids/cholesterol and specific proteins [2]. The lipid rafts have been isolated from several mammalian cells, mostly by their resistance to non-ionic detergent extraction and buoyancy on gradient ultracentrifugation. Studies from our group and others have shown that these methods performed with caution remain to be one of efficient approach to isolate and study the compositions of lipid rafts [3]. It was reported that ZGs and GP2 interact with the lipid raft

Abbreviations: DRM, detergent-resistant membrane; GPI, glycosylphosphatidylinositol; BSDL, bile salt dependent lipase; Nano-LC ESI Q-TOF MS/MS, nano liquid chromatography electrospray ionization in a quadrupole orthogonal acceleration time-of-flight mass spectrometry; SDS–PAGE, sodium dodecyl sulfate-polyacrylamide gel electrophoresis; SEM, standard error of the mean.

* Corresponding author. Address: Université Paul Cézanne, IMRN, UMR INRA 1111, LCBA , 13397 Marseille, France. Fax: +33 4 91 28 88 58.

E-mail address: a.hiol@univ.u-3mrs.fr (A. Hiol).

microdomains, and thus critical for the granule formation and protein secretion [4]. In this study, we have induced obesity in rat with high energy-starch diet (HESD) and the exocrine pancreas secretion response to diets was recorded. Lipid rafts from the exocrine pancreas were determined from either the ZG or PM. The proteome of the lipid rafts was simultaneously characterized by immunodetection and a proteomic approach including MALDI-TOF/MS and nano-LC ESI Q-TOF MS/MS. Among the 33 proteins that were identified included an important group of lipolytic proteins (pancreatic lipase, BSDL, lysophospholipase, and the co-lipase). Although the physiological relevance of these lipid rafts markers in the pancreas of obese rats needs further investigation, our data strongly indicate that these proteins may be involved in digestive, signaling, trafficking, and secretion functions of the pancreas.

Experimental procedures

Feeding protocols. Young male Sprague–Dawley rats were purchased from Elevage Janvier (Le Genest St Isle, France) in a post-weaning stage and kept under care in accordance with the principles of the guide for the care and use of experimental animals. After 1 week of adaptation under feeding with the standard diet A04 from Scientific Animal Food & Engineering (France), the rats (190–200 g) were divided into two groups. The control group was maintained under feeding with A04 (3.32 kcal/g) and the second group was fed with a HESD. The composition of the HESD (4.23 kcal/g) was casein (20%), lipids from vegetal oils (12%), methionine (0.3%), vitamins mix (1%), mineral mix (5%), fructose (10%), corn starch (47.2%), and sucrose (4.5%). The animals were weekly weighted and once in every 4 weeks monitored for blood glucose, cholesterol, triglyceride, and insulin levels after overnight fasting.

Rats exocrine pancreas response to diets. In standard experiment 16-weeks fed rats were fasted for 12 h before surgery. A PE-50 cannula was inserted into the right jugular vein for hormones infusion on animals anesthetized under the mixture of ketamine and xylazine at 60 mg/kg and 5 mg/kg, respectively. A midline incision of the abdomen was made then another cannula was placed in the distal end of the biliopancreatic duct. A ligature was placed around the common bile duct to collect the basal pure pancreas juice (PPJ). After 20 min collection of the pancreas fluid, CCK-8 and secretin in normal saline solution were infused at a rate of 0.25 μg/30 min, and the PPJ under the hormones stimulation was collected every 20 min. Pancreatic secretions were collected in a tube without or with 2–5 μl protease cocktail at 4 °C. The fluid volume was rapidly measured and the sample was saved in liquid nitrogen or at −80 °C. The protein concentration of the PPJ was determined and the amylase activity was measured using amylose as substrate [5]. The lipase activity was determined titrimetrically with olive oil emulsion in sodium taurocholate as substrate.

Isolation of zymogen granule and plasma membrane. After 16-weeks of feeding with AO4 or HSED, rats were fasted overnight prior to sacrifice. Trunk blood was collected for insulin and metabolite analysis. The pancreas were removed, weighted, and washed in homogenization buffer (HB) containing 20 mM Tris–HCl pH 8.2, 150 mM NaCl, 1 mM benzamidine, 1 mM PMSF, 250 μg/ml leupeptin, 1 mg/ml aprotinin, 1 mM pepstatin, and 5% sucrose. The tissue was excised into pieces, and homogenized HB with Ultra-Turrax T8 homogenizer and filtered through gauze then centrifuged at 500*g* for 10 min. One-half of the post-nuclear supernatant was centrifuged at 2000*g* for 10 min to pellet the ZG which was homogenized using Dounce homogenizer and ZG membranes were recovered by centrifugation at 10,000*g* for 30 min. The other half fraction was centrifuged at 2600*g* for 10 min and the pellet was suspended in HB and adjusted to 40% sucrose in a centrifuge tube and overlaid with HB. After centrifugation at 100,000*g* for 1 h, the floating membrane at the interface was collected and suspended in 4 volumes of HB (w/v) and membranes were pelleted and washed twice with HB. Activity of alkaline phosphatase activity and Na^+/K^+ ATPase was determined for PM enrichment [6].

Protein identifications by nano-LC ESI Q-TOF MS/MS. The in-gel digested peptides were analysed by nano-electrospray ionization (ESI) quadrupole time-of-flight (Q-TOF) MS/MS (nano-ESI-Q-TOF Ultima, Waters-Micromass, UK) coupled with a nano-liquid chromatography. The samples (1 μl) were loaded onto a pre-column reversed phase C18 in-line with a nano-column (Atlantis™ dC18 5/3 μm NanoEase™). Gradient elution was performed from 5% to 95% B for 136 min with A: 5% acetonitrile/0.1% formic acid; B: 95% acetonitrile/0.1% formic acid. The data acquisition of MS and MS/MS spectra were performed in a positive ion mode using the Micromass software Mass Lynx. Doubly and triply charged ions above a determined threshold were automatically selected and fragmented. Statistical studies were achieved using NEMROD Software [7]. Differences with $p < 0.05$ were considered statistically significant.

Results and discussion

High energy-starch diet induced obesity in Sprague–Dawley (SD) rats

The rise of obesity around the world in the past decades is greatly influenced by diet. Our initial investigation on the effects of the diet composition indicated that the SD rats fed with HESD diverged into two distinct groups based on body weight (BW) gain. The rats that gained the highest and lower weight under feeding with HESD were therefore designated as diet-induced obese (DIO) and obesity resistant (OR) rats, respectively. In contrast to the HESD, animals fed with the standard diet did not display significant difference based on BW gain. Although DIO rats exhibited the same BW compared to the control animal groups on standard diet after 6-weeks feeding (Fig. 1), the DIO gained more BW than the OR rats (446 ± 7 g vs 434 ± 4 g, $p < 0.01$). The food intake by DIO rats was about 1.5-fold compared to OR during the first 3 weeks feeding (data not shown). Similar assignment of rats into obese and lean

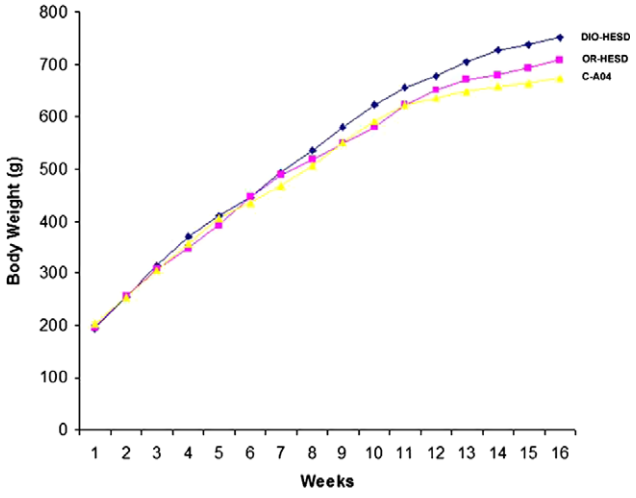

Fig. 1. Long term feeding with HESD induced a characteristic bimodal distribution of body weight. Outbred male Sprague–Dawley rats were fed for 16 weeks either with the control diet ($n = 12$) or the HESD ($n = 36$) ad libitum as described in feeding protocol.

groups was previously reported with the high-energy-fat diets [8,9]. It should be noted that the high-energy-fat diets have been associated with hyperphagia, therefore may induce obesity earlier than the carbohydrate based diets. A summary of parameters studied from the animals after 16-weeks feeding is given in Table 1. Based on the obesity

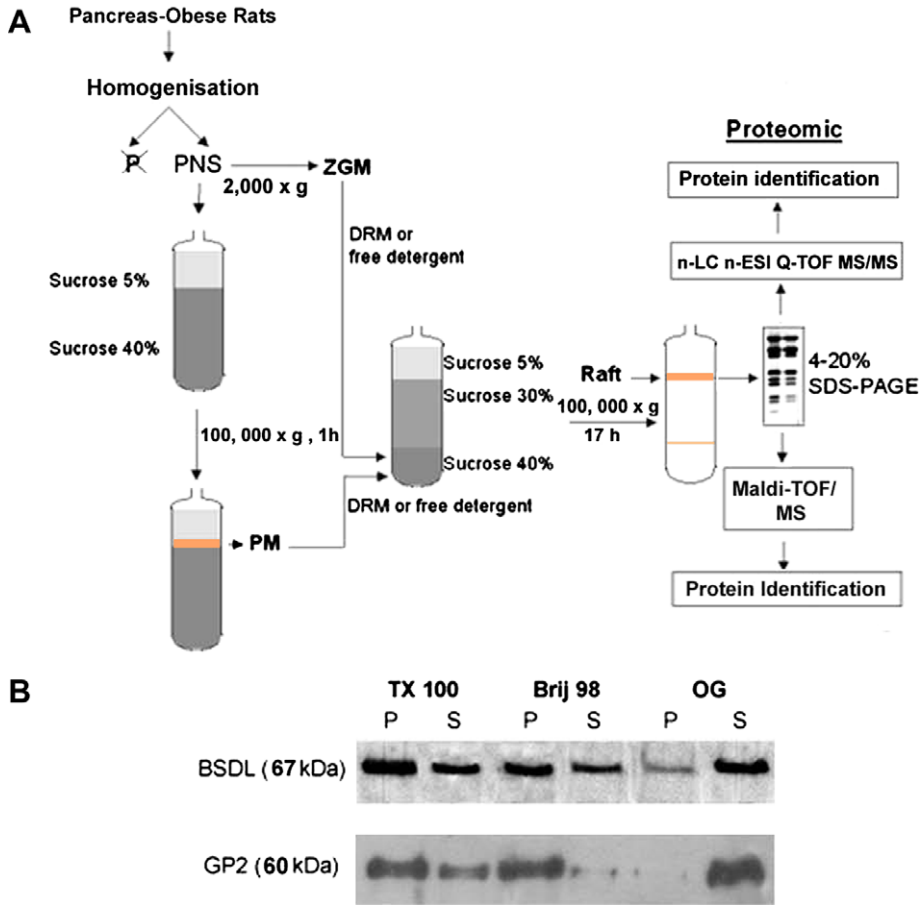

Fig. 2. Schematic overview of purification of lipid rafts from the exocrine pancreas of obese rats. (A) Flow chart illustrating the lipid rafts isolation. The ZGM, PM, and raft fractions were isolated by sub-cellular fractionation as described under experimental procedures. (B) BSDL and GP2 distribution in the DRMs. Total proteins (25 μg) from either ZM or PM were treated with detergents then the pellet (P) and supernatant (S) were tested by immunoblotted using the BSDL or GP2 specific antibody.

Table 1
Summary of effects after long term feeding with HESD in rats

	AO4	HESD-DIO	HESD-OR
BW (g)	673 ± 4	$751 \pm 5^{*}$	708 ± 7
Pancreas weight/BW	3.65×10^{-3}	3.31×10^{-3}	3.54×10^{-3}
Obesity index[a]	334 ± 1.23	$348 \pm 2.27^{*}$	340 ± 1.89
Plasma glucose (mmole/l)	7.39 ± 0.5	7.61 ± 0.2	6.72 ± 0.9
Cholesterol (g/l)	0.58 ± 0.05	$0.68 \pm 0.09^{**}$	0.61 ± 0.07
Triglycerides (g/l)	1.24 ± 0.08	$2.35 \pm 0.1^{*}$	1.39 ± 0.04
PPJ volume μl/20 min at 60 min[b]	180 ± 20	$220 \pm 15^{*}$	200 ± 20
Lipase SA[c]	28 ± 2	$111 \pm 5^{*}$	39 ± 3
Amylase SA[c]	98 ± 9	$209 \pm 14^{*}$	142 ± 11

After 16-weeks feeding with HESD body weight, length, and pancreas weight were measured. Blood sample was collected from each animal before sacrifice to estimate glucose, insulin, cholesterol, and triglyceride levels as described under Experimental procedures. Data are presented as means ± SE. $N = 12$–18 rats/group.

$^{**}p < 0.05$ and $^{*}p < 0.01$ for comparison between DIO and OR.

[a] Obesity index was calculated by dividing cubic root of the body weight and the length (mm) $\times 10^4$.

[b] Volume of the pancreas fluid collected in 20 min after 40 min of hormones infusion was initiated.

[c] The enzyme specific activity (SA) was defined as the release of 1 μmol of substrate/min/mg protein from the PPJ.

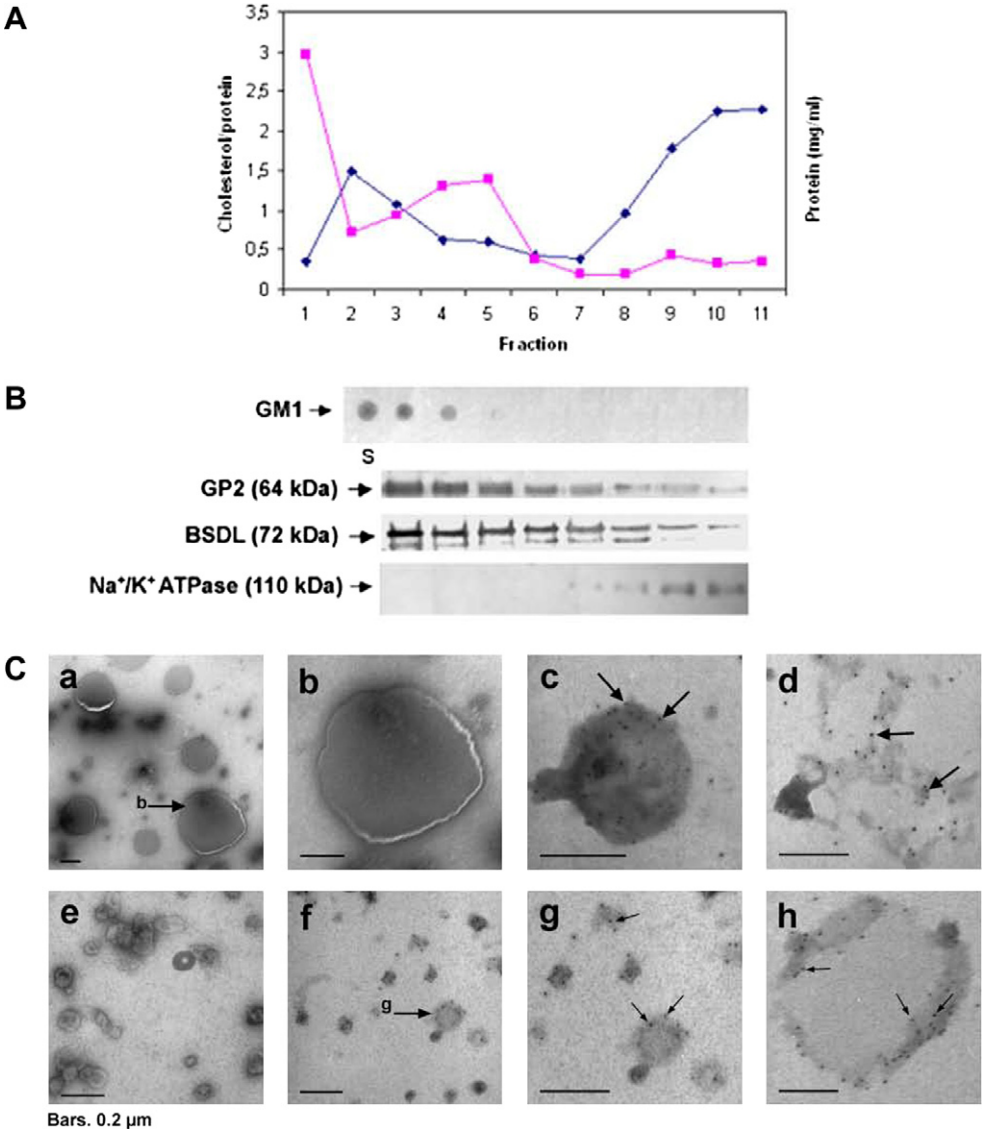

Fig. 3. Lipid rafts characterization. DRMs fractions were prepared from PM, and fractions were collected as described in experimental procedures. (A) The total protein and cholesterol content of each fraction was determined. (B) Equal total protein (10 µg) of every fraction was separated by 12.5% SDS–PAGE and immunoblotted with appropriate antibodies for BSDL, GP2, and Na^+/K^+ ATPase. For ganglioside GM1 blots were incubated with 1 µg HRP-cholera toxin B. The data are the representative of four experiments. (C) BSDL immunogold labeling of lipid raft vesicles. The LDFs (4–5) obtained either from the ZG or the PM were embedded for immunoelectron microscopy then incubated without (a, b, and e) or with the anti-BSDL antibodies (c, d, f, and g). Heterogeneous sizes of the rafts-like-vesicles with lining membrane are observed. The raft vesicles from the PM were smaller (e and f) and the intense labeling of the reverse membrane sheet particularly in (h) suggesting that the BSDL may be associated to one leaflet of membrane. Bars, 0.2 µm. Data shown are from DIO and no significant differences was noticed with OR.

index in rats [10], the DIO exhibited a significant increase of this parameter compared to OR and standard AO4 diet (348 ± 2.2 vs 340 ± 1.8 and vs 334 ± 1.2, $p < 0.01$). In order to determine the pancreas secretion response in relation to diets the PPJ volume, and the activities of lipase and amylase in PPJ were measured. Twenty minutes prior to hormones infusion, the same low volume of about 30 µl ± 5 was collected from each of the three groups and they exhibited similar lipase or amylase specific activities. In contrast to the basal conditions, following CCK-8/secretin stimulation, more than 160 µl of PPJ was recovered and the maximum secretion was obtained 40 min after hormone infusion (Table 1). As expected, lipase and amylase SA were increased in animals fed with HESD compared to AO4 groups. Remarkably, amylase and lipase specific activity (SA) were elevated in DIO compared to OR by 1.5- and 3-fold ($p < 0.01$), respectively. In contrast to PPJ, identical intracellular SA of lipase and amylase were measured in the pancreas extract from DIO and OR (data not shown). These results indicated that the differences between DIO and OR may be explained by the enzymes secretion of the pancreas in response to HESD. Fasting plasma glucose and insulin levels were similar between the three groups, whereas a significant increase of fasting

Table 2
Nano-LC ESI Q-TOF MS/MS identification of the lipid rafts proteins from the DIO rat exocrine pancreas

No.	Swiss-Prot-number	Identified protein	MW (kDa)	Score	Coverage (%)	Matched peptides	[a]R-PM
1	P19218	GP2	60	56	10	5	R-PM
2	P07882	BSDL	67	303	10	6	R-PM
3	P27657	Pancreatic lipase	52	367	24	8	R-PM
4	P54316	Pancreatic Lipase protein 1 precursor	53	40	5	2	R-PM
5	Q5SVC6	VDAC1	32	301	34	7	R-PM
6	P81155	VDAC2	32	248	25	5	R-PM
7	Q6GSZ1	VDAC3	31	215	29	6	R-PM
8	P15999	ATP synthase α	59	35	5	2	R-PM
9	Q499W0	ATP synthase β	56	84	8	3	R-PM
10	Q6NYBY	Rab1	23	67	10	2	R-PM
11	P35289	Rab15	24	67	10	2	R-PM
12	Q3U4W5	Rab6	23	53	5	1	R-PM
13	Q5U316	Rab35	23	67	10	2	R-PM
14	Q6P7A7	Ribophorin I	68	142	11	6	
15	P25235	Ribophorin II	63	74	9	4	
16	P67779	Prohibitin	30	258	32	7	R-PM
17	Q5XIH7	Prohibitin 2	33	234	23	6	R-PM
18	Q4V7D1	TRAP α	32	49	9	2	
19	Q08013	TRAP γ	21	76	7	1	
20	Q07984	TRAP δ	19	113	24	4	
21	Q641Y0	Protein glycosyltransferase	49	161	12	5	
22	Q63016	Integral membrane protein E16	56	31	2	1	R-PM
23	Q63584	Transmembrane protein Tmp 21	24	50	14	3	
24	Q6AYQ4	Transmembrane protein 109	26	72	4	1	
25	Q505I3	Sec61-α subunit	52	86	6	3	R-PM
26	Q4FZT0	Stomatin like 2	38	29	3	1	R-PM
27	P60711	Beta-actin	42	221	17	6	R-PM

[a] R-PM the positive hit was identified from both the ZG and purified PM lipid rafts. No significant difference in lipid rafts identification profile was noticed between DIO and OR animals.

blood triglyceride and cholesterol was observed in DIO rats. In another study an increase of plasma glucose and insulin were associated with a high-fat (45%) diet induced obesity in SD rats [9]. These discrepancies may be due to the differences among the SD phenotype strain and more importantly the calorie density or the composition of the diet. The high-energy diet selected here exhibited a calorie density of 4.23 kcal/g, of which 2.46 kcal/g from carbohydrates (78% starch). Using similar calorie density (3.93 kcal/g) of high-energy-carbohydrate diet but rich in sucrose instead of starch, the obese animals showed elevated blood insulin and triglyceride levels compared to the lean phenotype [11]. Together these results suggest that different forms of obesity could be generated by intake of food composition. We propose that the diet-induced obesity model developed here may be used to address BW regulation independently to the risk of morbidity from hypertension, diabetes 2, and stroke. Food composition and the regulation of the exocrine pancreas have been well-documented essentially for the soluble digestive enzymes. However, the dynamic membrane adaptation of exocrine pancreas dependent on the physiologic state induced by diet remains to be elucidated.

Purification of the lipid rafts from DIO and OR rats

In order to characterize the effect of HESD induced obesity on pancreas membrane, the exocrine pancreas of both DIO and OR rats were used to isolate the lipid rafts from either the ZGM or PM (Fig. 2A). Previously, immunoblotting of BSDL in the lipid rafts was reported in pancreatic SOJ-6 cells [12]. In order to isolate the DRMs, non-ionic detergent extraction was performed, and both BSDL and GP2 were partially extracted with TX-100 and Brij 98 but completely solubilized with OG (Fig. 2B). The low-density fractions (LDFs) on sucrose gradient isolated after extraction with TX-100 at 4 °C may not be an artifact of lipid complex induced by cold because similar distribution of BSDL and GP2 was obtained after Brij 98 treatment at 37 °C. The LDFs (4–5) were enriched in cholesterol and exhibited low total protein content (Fig. 3A). Using the HRP-conjugated cholera toxin B, the ganglioside GM1 was present in LDFs. while Na^+/K^+-ATPase, a PM protein not found in lipid rafts (6), was only detected in high-density fractions (HDFs) 9–11 (Fig. 3B). Additionally BSDL and GP2 were shown to be enriched in the LDFs (Fig. 3B). Treatment of the pancreas with 2% methyl-β-cyclodextrin for 30 min that reduced 37 ± 4% cholesterol in the LDFs and significantly shifted both BSDL and GP2 to HDFs (data not shown). Furthermore, as shown by morphology studies in Fig. 3C, the LDFs from the ZGM and PM exhibited rafts-like vesicles. Immunogold labeling of BSDL showed an intense staining on the membrane from the ZG and PM (Fig. 3C, d and g, respectively). These data strongly support that the LDFs isolated here exhibited most of the characteristics expected for the lipid rafts microdomains. A comprehensive proteome

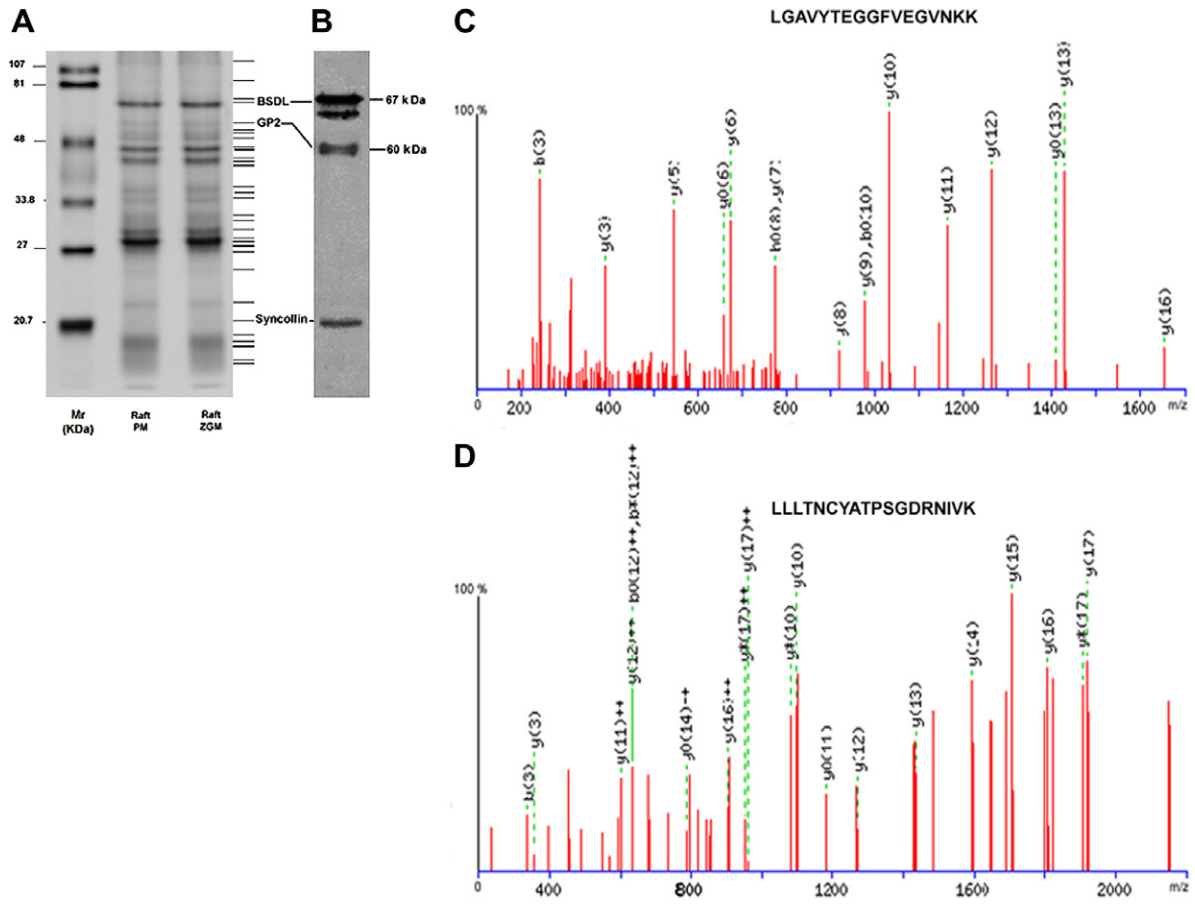

Fig. 4. Selected MS/MS peptide sequences. (A) Lipid rafts from the purified PM were isolated as described in the legend of Fig. 2A. Total protein (10 μg) of the LDFs were separated by 12% SDS–PAGE and silver staining bands were analyzed by proteomic. (B) Immunoblot of the indicated polypeptide with the specific antibody as described in the legend of Fig. 3. (C,D) MS/MS fragmentation spectra of LGAVYTEGGFVEGVNKK from (589.987500, 3^+) and LLLTNCYATPSGDRNDIVK from (717.353500, 3^+) leading to identification of BSDL (C) and GP2 (D), respectively.

profile of lipid rafts from the exocrine pancreas is needed to improve our understanding about potential roles of these microdomains in digestive enzymes regulation. However, due to high hydrophobic character and subsequent low solubilization, the resolution of lipid rafts protein separation in 2D gel electrophoresis was a challenge. Therefore, proteins from the lipid rafts were solubilized and separated in 1D gel.

Proteome characterization of the lipid rafts

In addition to the parameters we described previously [3], the main criteria for protein identification by MALDI-TOF/MS were the coverage of at least 24% and an expectation value <0.1 (Supplementary Table 1). Among 12 proteins identified, $G\alpha_q$ was an exception, because its expectation value >0.2, however was detected in raft fraction by immunoblotting (data not shown). Due to intracellular membranes contamination in particular from mitochondria and probably the lack of an efficient peptides separation with MALDI-TOF/MS analysis, only samples from PM provided a comprehensive proteome profile (Supplementary Table 1). In contrast to MALDI-TOF/MS, 27 proteins were identified in lipid rafts by nano-LC ESI Q-TOF MS/MS proteomic (Table 2). Nevertheless, some presumed mitochondrial proteins including ATP synthases α/β, channels, and trafficking proteins were found in the lipid rafts. Although the organelle contaminations from subcellular fractionations cannot be excluded, it should be noted that ATP synthases α/β have been reported to distribute in raft domains and were shown to localize in the PM of HepG2 hepatocytes by immunofluorescence [13]. Nineteen proteins (Table 2) were identified from lipid rafts prepare using the PM. Among them five proteins (GP2, BSDL, pancreatic lipase, ATP synthase β, and β-actin) were simultaneously identified by the MALDI-TOF/MS. These observations suggested that an elevated number of proteins are identified by a single approach, therefore combination of both methods can provide complementary results for rafts proteome studies. The low number of proteins identified by our proteomic approaches may be partly due to limited proteins reside in the lipid rafts. In agreement with the immunoblotting of GP2 and BSDL in the lipid rafts (Fig. 4B), the fragmented peptide spectra of LGAVYTEGGFVEGVNKK for BSDL (Fig. 4C) and LLLTNCYATPSGDRNDIVK for GP2 (Fig. 4D) are illustrated to confirm their identification. Sequencing pat-

tern of peptides leading to the identification of proteins in Table 2 is given in Supplementary Fig. 1. In contrast to GP2, syncollin previously described as lipid rafts protein of the ZGs [4] was not found by our proteomic analysis. However, immunoblotting using syncollin antibody showed the presence of syncollin in the LDF (Fig. 4B), suggesting that the rafts-associated syncollin may not be at least totally excluded from the gel separation. Using the iTRAQ labeling, a recent proteomic study of the whole zymogen membrane has distinguished the membrane from the so called non-membrane proteins group based on 117:114 ratio >1 and <1, respectively [14]. A significant number of the lipid rafts proteome found here was in agreement with their results. Furthermore, four of the proteins in Table 2 (3, 4, 8, and 9) belonged to the non-membrane, whereas 7 proteins (5, 6, 10, 12, 23, and 26) were classified as membrane proteins. It should be noted that based on the TMHMM transmembrane predication [15], up to 40% of the rafts proteins exhibited at least one transmembrane domain. Indicative for the validation of proteomic approaches, most of the proteins found in the lipid rafts can be taken as membrane or membrane-associated proteins. Finally, based on their presumed interactions and presumed functions, we propose that the proteins identified in the lipid rafts (Supplementary Table 2) may fall into at least four categories that include the lipolytic enzymes (2–4), transporters or channel proteins (5–9), signaling (10–13) and trafficking proteins (14–25). Combined with the MALDI-TOF/MS results, colipase or lysophospholipase may be added to the lipolytic group whereas $G\alpha_q$ and annexin II could be assigned in the signaling and trafficking group, respectively. How these digestive proteins may target to lipid rafts and the physiologic significance in relation with diet remains to be elucidated.

In conclusion, we developed an interesting form of obesity with a high-energy-starch diet in rats. Although the whole tract digestibility of intake food was not recorded between DIO and OR, the results from the exocrine pancreas response indicated that HESD increased pancreas fluid volume, amylase and in a more extent lipase SA in the DIO rats. The finding of lipid rafts proteins which were classified into functional groups may be crucial to provide new insights into the molecular mechanisms that underline the exocrine pancreas functions in relation to the diet.

Acknowledgments

A.A.B. and H.T.T.N. were supported by the French Government fellowships. This research has been facilitated by access to the Centre d'Analyse Protéomique de Marseille-Nice-Genopole®. The authors are especially grateful to Dr. Daniel Lafitte and Claude Villard (Plateau protéomique, Université de la Méditerranée, France) and to Dr. Michael Schrader (University of Marburg, Germany) for valuable discussions.

Appendix A. Supplementary data

Supplementary data associated with this article can be found, in the online version, at doi:10.1016/j.bbrc.2007.02.037.

References

[1] A. Ben Abdeljlil, A.M. Visani, P. Desnuelle, Adaptation of exocrine secretion of the rat pancreas to the composition of the diet, Biochem. Biophys. Res. Commun. 10 (1963) 112–116.
[2] D.A. Brown, E. London, Structure and function of sphingolipid- and cholesterol-rich membrane rafts, J. Biol. Chem. 275 (2000) 17221–17224.
[3] H.T.T. Nguyen, A.A. Berkane, D. Lafitte, A.A. Waheed, C. Nicoletti, C. Villard, M. Létisse, V. Deyris, M. Rozière, L. Tchiakpe, D. Comeau-Druet, L. Comeau, A. Hiol, Proteomic characterization of lipid rafts markers from the rat intestinal brush border, Biochem. Biophys. Res. Commun. 342 (2006) 236–244.
[4] K. Schmidt, M. Schrader, H.-F. Kern, R. Kleene, Regulated apical secretion of zymogens in rat pancreas. Involvement of the glycosylphosphatidylinositol-anchored glycoprotein GP-2, the lectin ZG16p, and cholesterol-glycosphingolipid-enriched microdomains, J. Biol. Chem. 276 (2001) 14315–14323.
[5] N. Oudjeriouat, Y. Moreau, M. Santimone, B. Svensson, G. Marchis-Mouren, V. Desseaux, On the mechanism of α-amylase acarbose and cyclodextrin inhibition of barley amylase isozymes, Eur. J. Biochem. 270 (2003) 3871–3879.
[6] A. Hiol, J.M. Caron, C.D. Smith, T.L. Jones, Characterization and partial purification of protein fatty acyltransferase activity from rat liver, Biochim. Biophys. Acta 1635 (2003) 10–19.
[7] D. Mathieu, J. Nony, R. Phan-Tan-Luu, New efficient methodology for research using optimal design (NEMROD) software, LPRAI, Marseille, France, 2000.
[8] B.E. Levin, A.A. Dunn-Meynell, B. Balkan, R.E. Keesey, Selective breeding for diet-induced obesity and resistance in Sprague–Dawley rats, Am. J. Physiol. Regul. Integr. Comp. Physiol. 273 (1997) R725–R730.
[9] E.E. Otukonyong, M.G. Dube, R. Torto, P.S. Kalra, S.P. Kalra, High-fat diet-induced ultradian leptin and insulin hypersecretion are absent in obesity-resistant rats, Obes. Res. 13 (2005) 991–999.
[10] A.D. Dobrian, S.D. Schriver, T. Lynch, R.L. Prewitt, Effect of salt on hypertension and oxidative stress in a rat model of diet-induced obesity, Am. J. Physiol. Renal Physiol. 285 (2003) F619–F628.
[11] J.T. Dourmashkin, G.Q. Chang, E.C. Gayles, J.O. Hill, S.K. Fried, C. Julien, S.F. Leibowitz, Different forms of obesity as a function of diet composition, Int. J. Obes. (Lond.) 29 (2005) 1368–1378.
[12] E. Aubert-Jousset, N. Garmy, V. Sbarra, J. Fantini, M. Sadoulet, D. Lombardo, The combinatorial extension method reveals a sphingolipid binding domain on pancreatic bile salt-dependent lipase: role in secretion, Structure 12 (2004) 1437–1447.
[13] T.J. Bae, M.S. Kim, J.W. Kim, B.W. Kim, H.J. Choo, J.W. Lee, K.B. Kim, C.S. Lee, J.H. Kim, S.Y. Chang, C.Y. Kang, S.W. Lee, Y.G. Ko, Lipid raft proteome reveals ATP synthase complex in the cell surface, Proteomics 4 (2004) 3536–3548.
[14] X. Chen, A.K. Walker, J.R. Strahler, E.S. Simon, S.L. Tomanicek-Volk, B.B. Nelson, M.C. Hurley, S.A. Ernst, J.A. Williams, P.C. Andrews, Organellar proteomics: analysis of pancreatic zymogen granule membranes, Mol. Cell Proteomics 5 (2006) 306–312.
[15] A. Krogh, B. Larsson, G. von Heijne, E.L.L. Sonnhammer, Predicting transmembrane protein topology with a hidden Markov model: application to complete genomes, J. Mol. Biol. 305 (2001) 567–580.